Journal of Clinical Immunology (2019) 39:207–215
https://doi.org/10.1007/s10875-019-00606-7

ORIGINAL ARTICLE

Alternative Splicing Rescues Loss of Common Gamma Chain Function and Results in IL-21R-like Deficiency

David Illig[1] · Marta Navratil[2,3] · Jadranka Kelečić[4] · Raffaele Conca[1] · Iva Hojsak[3,5,6] · Oleg Jadrešin[5] · Marijana Ćorić[7] · Jurica Vuković[8] · Meino Rohlfs[1] · Sebastian Hollizeck[1] · Jens Bohne[9] · Christoph Klein[1] · Daniel Kotlarz[1]

Received: 12 December 2018 / Accepted: 25 February 2019 / Published online: 21 March 2019

Abstract

Inborn errors in interleukin 2 receptor, gamma (*IL2RG*) perturb signaling of the common gamma chain family cytokines and cause severe combined immunodeficiency (SCID). Here, we report two brothers suffering from chronic cryptosporidiosis, severe diarrhea, and cholangitis. Pan T, B, and NK cell numbers were normal, but immunophenotyping revealed defective B cell differentiation. Using whole exome sequencing, we identified a base pair deletion in the first exon of *IL2RG* predicted to cause a frameshift and premature stop. However, flow cytometry revealed normal surface expression of the IL-2Rγ chain. While IL-2, IL-7, and IL-15 signaling showed only mild defects of STAT5 phosphorylation in response to the respective cytokines, IL-4- and IL-21-induced phosphorylation of STAT3 and STAT6 was markedly reduced. Examination of RNA isoforms detected alternative splicing downstream of *IL2RG* exon 1 in both patients resulting in resolution of the predicted frameshift and 16 mutated amino acids. *In silico* modeling suggested that the IL-2Rγ mutation reduces the stabilization of IL-4 and IL-21 cytokine binding by affecting the N-terminal domain of the IL-2Rγ. Thus, our study shows that *IL2RG* deficiency can be associated with differential signaling defects. Confounding effects of alternative splicing may partially rescue genetic defects and should be considered in patients with inborn errors of immunity.

Keywords SCID · immunodeficiency · IL-21R · IL-2R · splicing

Introduction

Severe combined immunodeficiency (SCID) is a rare disease characterized by the absence of functional T cells and can be immunologically sub-grouped based on the presence or absence of B and NK cells ($T^-B^+NK^+$, $T^-B^-NK^+$, $T^-B^+NK^-$, and $T^-B^-NK^-$ forms) [1]. Clinically, SCID often manifests with failure to thrive and recurrent infections of the respiratory

Christoph Klein and Daniel Kotlarz contributed equally to this work.

Electronic supplementary material The online version of this article (https://doi.org/10.1007/s10875-019-00606-7) contains supplementary material, which is available to authorized users.

✉ Daniel Kotlarz
daniel.kotlarz@med.uni-muenchen.de

[1] Dr. von Hauner Children's Hospital, Department of Pediatrics, University Hospital, LMU Munich, Lindwurmstrasse 4, 80337 Munich, Germany

[2] Department of Pulmonology, Allergology, Rheumatology and Clinical Immunology, Children's Hospital Zagreb, Zagreb, Croatia

[3] School of Medicine, University J.J. Strossmayer, Osijek, Croatia

[4] Department of Pediatrics, Division of Clinical Immunology, Allergology, Respiratory Diseases and Rheumatology, University Hospital Centre Zagreb, Kišpatićeva 12, Zagreb 10000, Croatia

[5] Referral Center for Pediatric Gastroenterology and Nutrition, Children's Hospital Zagreb, Zagreb, Croatia

[6] School of Medicine, University of Zagreb, Zagreb, Croatia

[7] Department of Pathology and Cytology, University Hospital Centre Zagreb, Zagreb, Croatia

[8] Division of Pediatric Gastroenterology, Hepatology and Nutrition, University Hospital Centre Zagreb, Zagreb, Croatia

[9] Institute for Virology, Hannover Medical School, Hannover, Germany

and gastrointestinal tract [2, 3]. Early diagnosis of SCID is critical. Without adequate therapy (i.e., allogeneic hematopoietic stem cell transplantation or hematopoietic stem cell gene therapy), patients often die within the first year of life [1]. To date, more than 20 different monogenic defects were shown to cause SCID [4]. Loss-of-function mutations in these known candidates can result in heterogeneous phenotypes, since affected genes are involved in regulating different cellular mechanisms such as B and T cell receptor rearrangement (e.g., *RAG1*, *RAG2*, *PRKDC*) and immune cell signaling (e.g., *CD45*, *ADA*, *JAK3*, *IL7R*, *IL2RG*) [1, 4].

Approximately 50% of reported cases are caused by mutations in the *IL2RG* gene resulting in X-linked SCID (X-SCID) [5]. The common gamma chain (IL-2Rγ, γ_c) encoded by *IL2RG* is the shared receptor subunit for cytokines of the γ_c family (IL-2, IL-4, IL-7, IL-9, IL-15 and IL-21) and has a critical role in regulating development and function for a variety of immune cell types [6]. Most missense and especially frameshift and splice region mutations affecting the *IL2RG* are known to cause severe forms of SCID [7]. However, atypical forms of SCID with normal to low frequencies of T and NK cells can be observed. In these patients, a variety of mechanisms including hypomorphic mutations, spontaneous somatic reversion in T cell clones, or maternal engraftment of T cells have been reported [8–11]. Hypomorphic SCID with non-specific symptoms is particularly challenging, since clinical and molecular diagnosis may be masked and patients may be at risk for fatal complications [4, 9–11]. Advances in neonatal screening programs and next-generation sequencing facilitate an unbiased genetic investigation allowing early diagnosis and treatment of SCID cases. Here, we report two related patients with hypomorphic SCID and differential alterations of cytokine signaling caused by a novel mutation in the *IL2RG* gene that displays complexities in RNA splicing and consecutive cytokine signaling pathways.

Methods

Patients

Both patients were admitted and treated in the Children's Hospital Zagreb and University Hospital Centre Zagreb, Zagreb, Croatia. Blood samples were acquired upon written consent. The study and experiments were performed according to the current legal and ethical statutes and were approved by the institutional review board at the University Hospital, LMU Munich, and were in accordance with the ethical standards of the 1964 Helsinki declaration and its later amendments.

DNA Sequencing

Genomic DNA was extracted from peripheral blood donated by patients, parents, and the healthy sibling using QIAamp DNA blood mini kit (QIAGEN) according to the manufacturer's instructions. Whole exome sequencing on an Illumina NextSeq500 and variant calling for rare sequence variants following a Mendelian inheritance pattern was performed as previously described [12]. The *IL2RG* mutation and segregation with the disease phenotype was confirmed by Sanger sequencing using the following primer pairs: forward 5′-TACCACCTTACAGCAGCACC-3′; reverse 5′-CCCT TCCCACTCCACTTTTCA-3′. Sequencing analysis of gDNA or cDNA was analyzed using SeqMan Pro Software (DNASTAR Lasergene).

Immunophenotypical Analysis

After washing blood samples once with PBS, blood cells were stained with fluorescently labeled monoclonal antibodies as described previously [12]. Using FACS Lysing Solution (BD), erythrocytes were lysed following the manufacturer's instructions. The samples were acquired on a LSRFortessa Flow Cytometer (BD Biosciences), and data were analyzed using FlowJo software (TreeStar).

Analysis of Protein Expression of Mutated IL-2Rγ

For analysis of IL-2Rγ protein expression, 1×10^6 EBV-immortalized cells were lysed in cell lysis buffer (Cell Signaling Technology) supplemented with phenylmethanesulfonyl fluoride (AlphaDiagnostics) and protease inhibitor cocktail (Sigma) for 1 h on ice. To assess the glycosylation of IL-2Rγ, lysates were treated with PNGase F (NEB) according to manufacturer's instructions and deglycosylated at 37 °C for 2 h. Control samples were treated equally without addition of PNGase F. Proteins were separated under reducing conditions by SDS-PAGE and transferred to PVDF membranes using the Mini Trans-Blot® Cell (Bio-Rad) system. Unspecific binding of antibodies was blocked using 5% milk powder (Carl Roth) in PBS. IL-2Rγ was stained using IL-2Rγ Polyclonal Antibody (Thermo Fisher Scientific, #PA5–26461) and HRP goat anti-mouse IgG (Biolegend, #405306) and detected using SuperSignal West Pico Plus Chemiluminescent Substrate (Thermo Fisher Scientific) on a ChemiDoc XRS+ System (Bio-Rad).

To investigate surface expression of mutated IL-2Rγ, 0.5×10^6 EBV-immortalized cells from patients, first-degree relatives, and healthy donors were stained using anti-CD132 (BD Pharmingen, Clone: AG184, #555900) and analyzed by flow cytometry.

Phospho Flow

For analysis of IL-2Rγ-mediated signaling pathways, peripheral blood mononuclear cells (PBMCs) were isolated by density gradient centrifugation using Ficoll (GE Healthcare). 1×10^6 PBMCs per condition were resuspended in plain RPMI medium (Gibco) and incubated at 4 °C for 15 min. Cells were stimulated for 0, 5, 10, or 30 min at 37 °C with IL-2 (100 ng/mL), IL-4 (100 ng/mL), IL-7 (100 ng/mL), IL-15 (10 ng/mL), or IL-21 (50 ng/mL, all purchased from Peprotech). Stimulated cells were fixed using 4% paraformaldehyde in PBS (Santa Cruz) for 3 min at room temperature and permeabilized with ice cold methanol (Carl Roth) for 10 min on ice. Cells were stained with anti-CD3 (Pacific Blue, BD, #344824), anti-pSTAT3 (Y705, AF488, BD, Clone: 4/P-STAT3, #557814), anti-pSTAT5 (Y694, PE-CF594, BD, Clone: 47/Stat5(pY694), #562501), anti-pSTAT6 (Y641, unconjugated, Cell Signaling Technologies, #9361S), and anti-rabbit IgG (AF644, Thermo Fisher Scientific, #A11008). Samples were detected on a LSRFortessa Flow Cytometer (BD Biosciences), and data were analyzed using FlowJo software (TreeStar).

Analysis of IL-2Rγ-Mediated Protein Phosphorylation

For analysis of IL-2- and IL-21-mediated signaling, 1.0×10^6 PBMCs or 0.5×10^6 patient-derived EBV-LCLs were resuspended in plain RPMI (Gibco) and serum starved for 4 h or 18 h at 37 °C, respectively. Cells were stimulated for 0, 10, or 30 min at 37 °C with IL-2 (100 ng/mL) or IL-21 (50 ng/mL, both purchased from Peprotech). Stimulation was stopped by addition of ice-cold 2 mM sodium orthovanadate (Na_3VO_4, Sigma) in PBS. Cells were lysed in cell lysis buffer (Cell Signaling Technology) supplemented with phenylmethanesulfonyl fluoride (AlphaDiagnostics), protease inhibitor cocktail (Sigma), and Na_3VO_4 for 1 h on ice. Proteins were separated under reducing conditions by SDS-PAGE and transferred to PVDF membranes using the Mini Trans-Blot® Cell (Bio-Rad) system. Unspecific binding of antibodies was blocked using 5% BSA (Sigma) in PBS. p-STAT5 (pY694), p-STAT3 (pY705), STAT5, STAT3, and β-actin were stained using the antibodies summarized in Supplemental Table 1. For detection of chemiluminescence signals, we used the SuperSignal West Dura Extended Duration Substrate (Thermo Fisher Scientific) and ChemiDoc XRS+ System (Bio-Rad).

RNA Expression Analysis

Total RNA of 1×10^6 EBV-LCLs was prepared using RNeasy Plus Mini Kit (QIAGEN), and cDNA was generated using the High-Capacity cDNA Reverse Transcription Kit (Thermo Fischer Scientific) according to the manufacturer's instructions. Exon 1 to 3 of *IL2RG* cDNA were amplified by PCR using the following primers: forward 5′-GAGC AAGCGCCATGTTGAAGC-3′, reverse #1 5′-ACCC CAGGGGATCACCAGATT-3′ or reverse #2 5′-AGAT AGTGGCTGCACTTCTGGAC-3′. Amplified fragments were separated by agarose gel electrophoresis, and DNA was purified using QIAquick Gel Extraction Kit (QIAGEN) according to the manufacturer's instructions.

Quantitative expression of *IL2RG* mRNA was analyzed by qRT-PCR using FAST SYBR Green Master Mix and *IL2RG* exon-specific primers (Supplemental Table 2) on a StepOnePlus Real-Time PCR System (Thermo Fisher Scientific) according to the manufacturer's instructions. Fold changes were calculated using the $\Delta\Delta C_T$ method and the StepOne Software (Thermo Fisher Scientific). Expression of alternative transcripts was normalized to total *IL2RG* expression.

In Silico Modeling

Wild-type and mutant IL-2Rγ were *de novo* modeled using NovaFold and Protean 3D software (DNASTAR Lasergene) and superimposed to known crystal structures of IL-2 [13], IL-4 [14], and IL-15R [15] complexes using PyMol software (DeLano Scientific LLC, Schrödinger).

Statistical Analysis

For statistical testing, *t* tests with the Holm-Sidak method for correction of multiple comparisons were performed using Prism software (Version 6, GraphPad). Results were considered to be significant, if $p < 0.05$.

Data Availability

The *IL2RG* mutation identified in our patients is deposited in the ClinVar database (https://www.ncbi.nlm.nih.gov/clinvar/; ClinVar accession: SCV000882837). To ensure study participant privacy, raw whole-exome sequencing data will not be published.

Results

Clinical Description of Patients

In our study, two brothers born to non-consanguineous parents of Romani descent were referred to the Children's Hospital Zagreb for gastroenterological and immunological workup due to a disease reminiscent of IL-21R deficiency [16] with cryptosporidiosis, severe diarrhea, and cholangitis (Fig. 1a).

The 4-year-old index patient P1 presented with recurrent respiratory tract infections (viral infections, otitis media,

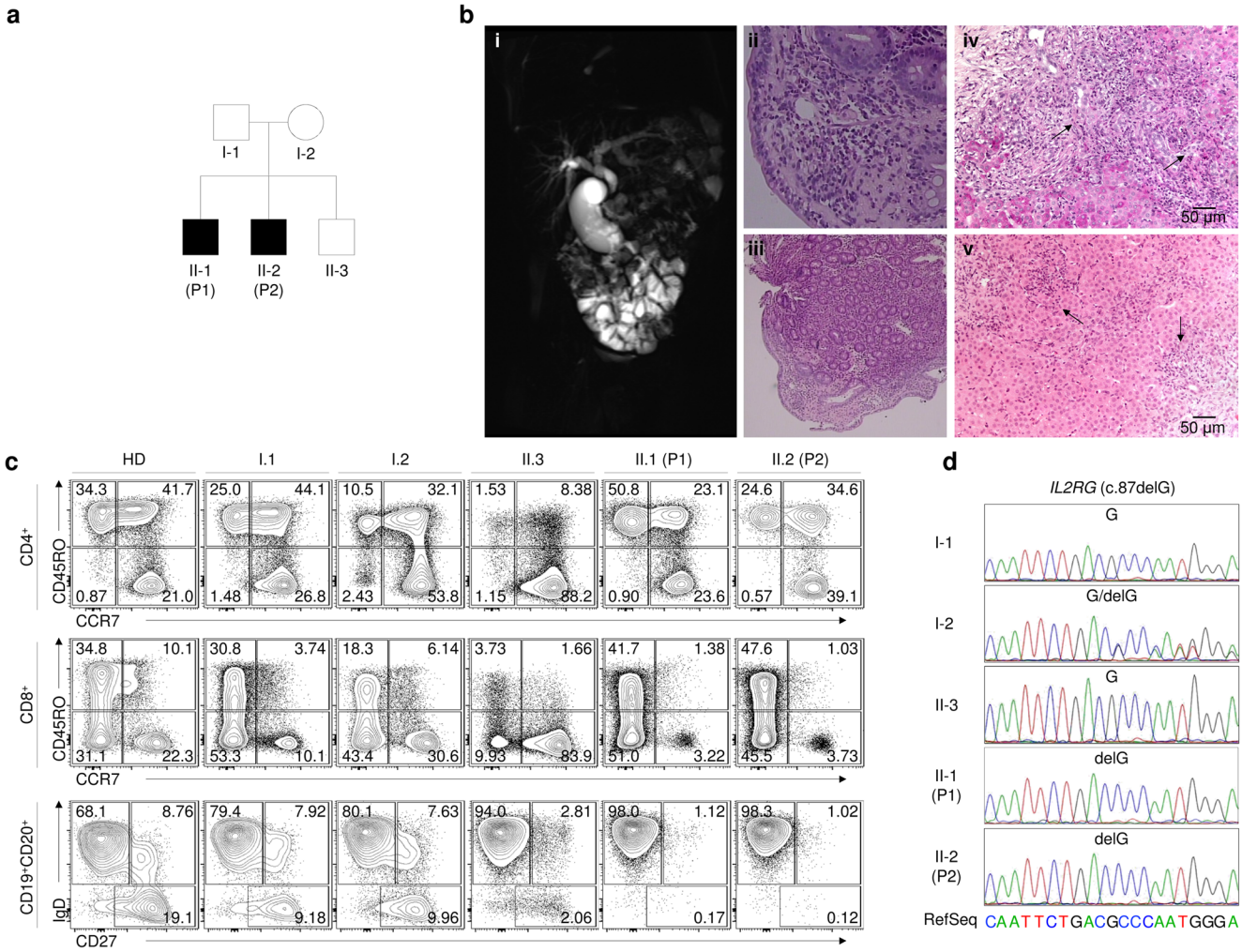

Fig. 1 Identification of an *IL2RG* mutation causing hypomorphic SCID with an IL-21R-like phenotype. **a** Pedigree of the index family with two patients suffering from chronic cryptosporidiosis. **b** Magnetic resonance cholangiography showed hepatosplenomegaly with dilatation of the hepatic ducts and ductus choledochus in patient P1 (II-1) (i). Histology of small intestinal mucosa of P1 revealed shortened villi and polymorphic infiltration in the lamina propia with abundance of lymphocytes, plasma cells, eosinophils, and mastocytes (ii, iii). PAS (iv) and H&E (v) staining of liver biopsies from P1 showing abundant chronic inflammatory infiltrates in portal spaces and proliferation of the bile ducts with mononuclear cells invading the walls of the bile ducts. **c** Detailed immunophenotyping of $CD4^+$ and $CD8^+$ T cells as well as IgD^+CD27^+ marginal zone and IgD^-CD27^+ class-switched B cells in peripheral blood from an unrelated healthy donor (HD), father (I-1), mother (I-2), the unaffected sibling (II-3), and both patients (II-1 and II-2). **d** Analysis of the segregation of the identified *IL2RG* mutation (c.87delG) with the disease phenotype in the index family

sinusitis, and bacterial pneumonia), failure to thrive, and chronic diarrhea since the age of 6 months. Abdominal ultrasound and magnetic resonance cholangiography showed hepatomegaly and dilatation of the hepatic ducts and ductus choledochus at the age of 4 years (Fig. 1b). Imaging findings were suggestive for cryptosporidial infection of the biliary tract, and *Cryptosporidum species* were detected in stool samples. Liver biopsy revealed cholangitis, chronic inflammatory infiltrates, and macro- and microvesicular steatosis (Fig. 1b). At the age of 4.5 years, P1 developed arthritis of the left elbow and interphalangeal joints of both hands as well as disseminated skin granulomas with centers rich in eosinophils and necrotic debris.

His 2.5-year-old brother Patient 2 (P2) had reportedly recurrent viral respiratory tract infections, otitis media, and sinusitis as well as soft and frequents stools since birth. He was treated by surgical drainages due to perianal abscesses within the first months of life. Similar to P1, he showed hepatosplenomegaly as well as dilatation and structural alterations of the bile duct system at the age of 2 years.

Routine immunological analysis showed normal or increased numbers of $CD3^+$ T (P1 5.788; P2 2.355; normal range 1.32–3.3 × 10^9/L), $CD19^+$ B (P1 0.847; P2 1.081; normal range 0.27–2.050 × 10^9/L), and $CD16^+CD56^+$ NK (P1 0.353; P2 0.309; normal range 0.19–0.74 × 10^9/L) cells. However, both patients showed increased numbers of $CD8^+$ T cells (P1 3.529; P2 1.853;

normal range 0.39–1.1 × 10^9/L), while $CD4^+$ cells were reduced in P2 and normal in P1 (P1 1.482; P2 0.232; normal range 0.62–2.4 × 10^9/L) resulting in inversed $CD4^+$/$CD8^+$ T cell ratios (P1 0.32; P2 0.125; norm 0.9–3.1). Based on the expression of CD45RO and CCR7, detailed immunophenotyping of PBMC revealed overall normal differentiation of $CD4^+$ and $CD8^+$ T cells in both patients (Fig. 1c). Frequencies of patients' $CD127^-CD25^+$ Treg cells, $CCR6^-CXCR3^+$ T helper 1 (Th1), $CCR6^+CXCR3^-$ Th17, and $CCR6^-CXCR3^-$ double negative Th2-enriched cells were normal (data not shown). T cell proliferation was slightly reduced in response to phytohemagglutinin (P1 16; P2 10; normal >17) and concanavalin A (P2 6; normal > 7). HIV infection was excluded in both patients. Notably, B cell differentiation was severely impaired in both children, as indicated by substantial reduction of $CD19^+CD20^+IgD^+CD27^+$ marginal and absent $CD19^+CD20^+IgD^-CD27^+$ class-switched B cells (Fig. 1c). Analysis of immunoglobulin levels revealed increased IgM and IgA levels in both patients. In addition, P1 showed increased total IgG and IgE levels, while IgG1 and IgG2 subclasses were decreased (P1: IgG1 1.77 g/L, reference value 3.62–12.28 g/L; IgG2 < 0.34 g/L, reference value 0.57–2.9 g/L). Corresponding to the IgE serum level, we could observe increased absolute numbers of eosinophils only in P1, but increased relative frequencies in both patients (P1 2.54 × 10^9/L, 13%; P2 0.4 × 10^9/L, 9%; reference value < 0.7 × 10^9/L, < 6%). Both patients showed an absent antibody response to hepatitis B and morbilli-parotitis-rubella immunization.

Initial treatment of both patients included IVIG substitution (600 mg/kg every month), azithromycin (20 mg/kg daily), trimethoprim/sulfamethoxazole (*Pneumocystis jiroveci pneumonia* prophylaxis), ursodeoxycholic acid, vitamin supplements, and hypercaloric enteral nutrition. In the absence of an HLA-identical hematopoietic stem cell donor, definitive therapy by haploidentical HSCT using the mother as donor has been attempted. However, P1 died 60 days post-HSCT at the age of 6 years due to GVHD complications and P2 succumed to infectious complications 60 days post-HSCT at the age of 4 years.

Rescue of the IL2RG Loss-of-Function Mutation by Alternative Splicing

To discover the underlying molecular pathology, we conducted whole exome sequencing of both patients. Bioinformatics analysis showed a hemizygous mutation in the first exon of *IL2RG* (ENST00000374202, X:70331302–70331303, c.87delG, p.Asn31MetfsTer12) predicted to cause a frameshift and premature stop in exon 2. Sanger sequencing confirmed segregation of the identified mutation with the disease phenotype, because the mother (I-2) was heterozygous and the father (I-1) as well as the healthy sibling (II-3) had a hemizygous wild-type genotype (Fig. 1d). In view of the unusual phenotype, we decided to further investigate the molecular details of the mutation by functional assays. Analysis of mRNA expression by qRT-PCR revealed no differences in *IL2RG* expression between the patients, first degree relatives, and healthy controls (Fig. 2a). Unexpectedly, immunoblotting and flow cytometric analysis suggested a normal surface expression of IL-2Rγ protein in patients' EBV-LCL (Fig. 2b).

Different mechanisms to bypass frameshift mutations have been reported, including alternative start sites and splicing [17, 18]. The predicted transcript *IL2RG*-002 in the *Ensembl genome database* indicated a possible alternative splice site 28 bp downstream of exon 1 (Fig. 2c). The usage of this site has been previously shown in the context of an *IL2RG* mutation that disrupted the 3′ splice site of exon 1 and resulted in a non-sense transcript and loss of protein expression [19]. Based on these data, we hypothesized that the frameshift could be resolved by alternative splicing mechanisms in intron 1 of *IL2RG* (Fig. 2d). Bioinformatics analysis suggested that the alternative splice site creates a premature stop codon in wild-type *IL2RG* but leads to restoration of a productive version of *IL2RG* mRNA starting from exon 2 in combination with the identified base pair deletion c.G87 (Fig. 2d). The protein is predicted to have 16 mutated amino acids due to the frameshift and splicing downstream of exon 1, whereas the amino acid sequence of the signal peptide, transmembrane domain, and signaling domain of IL2Rγ remain unchanged (Fig. 2d). To assess this hypothesis, we generated cDNA from EBV-LCL and amplified the fragment between exon 1 and exon 3 or 4, respectively. Using agarose gel electrophoresis, we could detect an additional fragment for both patients corresponding to the expected size of the predicted alternative transcript (Fig. 2e). Sequencing of the amplified cDNA fragments confirmed the presence of a hemizygous deletion for both patients (Fig. 2e). Moreover, we could detect two distinct reads downstream of exon 1 in both patients that matched (a) the sequence of canonical spliced exon 2 and (b) the intronic region, indicating the use of both canonical and alternative splice sites during mRNA maturation of mutated *IL2RG* (Fig. 2e). qRT-PCR analysis revealed the presence of the alternative sequence in all tested donors; however, both patients showed increased expression of the alternative sequence, suggesting a stronger usage of the alternative splice site (Fig. 2f).

Differentially Impaired Cytokine Signaling in IL2RG Deficiency

To assess the functional consequences of the IL-2Rγ mutation, we analyzed the signal transduction of patients' PBMC in response to common gamma chain cytokines IL-2, IL-4, IL-7, IL-15, or IL-21 by phospho-flow. While STAT5 activation showed only mild or no abnormalities in response to IL-2, IL-7, and IL-15, phosphorylation of STAT3 in response to IL-21 was significantly reduced in patients' $CD3^+$ and $CD3^-$ cells, as compared to HD and parents (Fig. 3a). Defective IL-21-mediated signaling was confirmed independently by

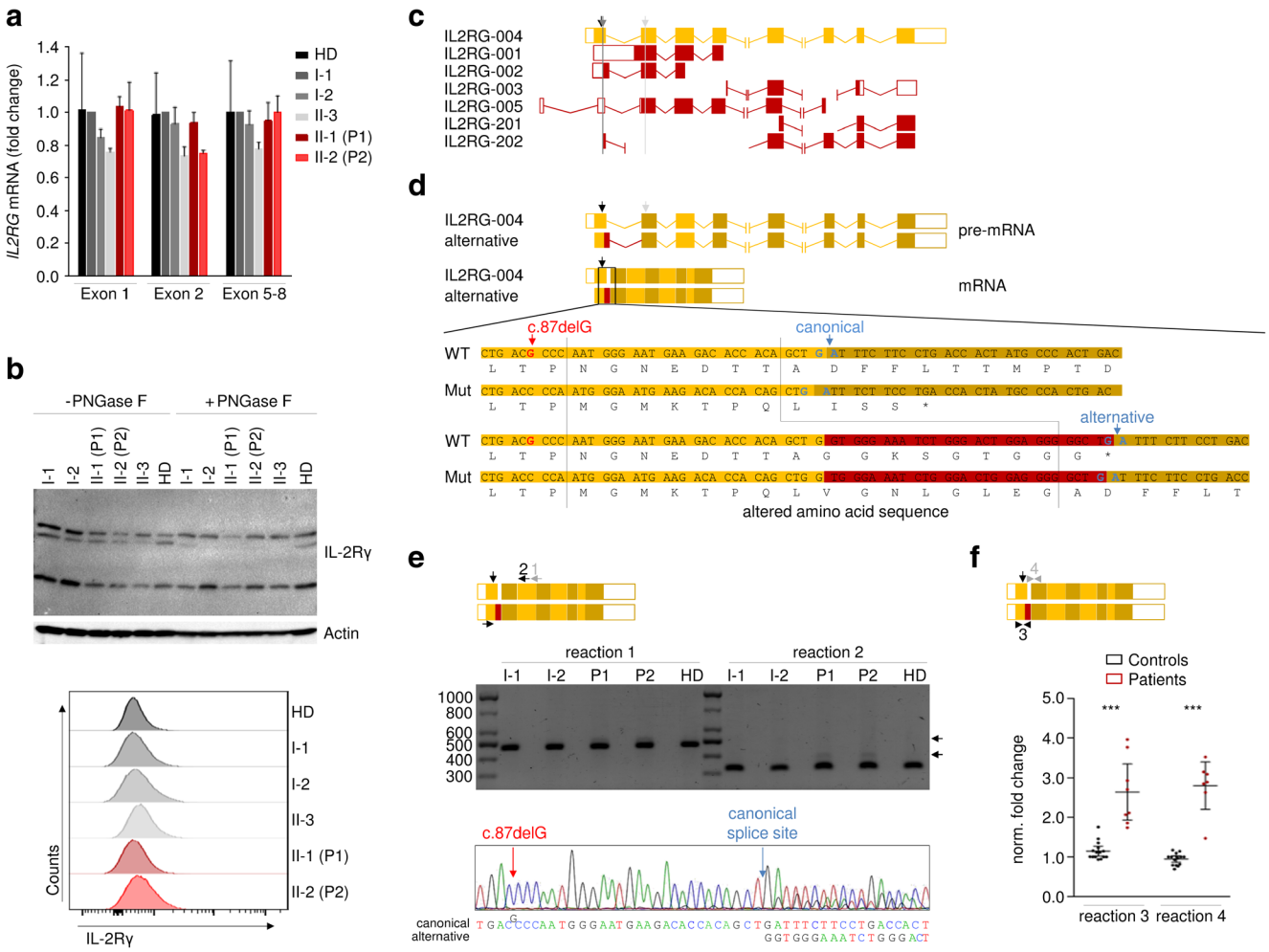

Fig. 2 Alternative splicing resolves loss of IL-2Rγ expression and function. **a** Analysis of *IL2RG* mRNA expression in EBV-LCL from unrelated donors (HD), father (I-1), mother (I-2), the unaffected sibling (II-3), and both patients (II-1 and II-2) by qRT-PCR (3 independent experiments). **b** Representative immunoblotting (n=3) and FACS ($n = 2$) of IL-2Rγ protein expression in EBV-LCLs. **c** Schematic overview of predicted *IL2RG* transcripts based on information from the *Ensemble genome database*. **d** Predicted consequence of the *IL2RG* mutation and alternative splicing on the amino acid sequence. **e** cDNA amplification and sequencing of the mutated *IL2RG* transcript with two different PCR reactions: (1) exon 1–4, (2) exon 1–3. Representative cDNA sequencing of the larger PCR product from EBV-LCL in patient II-2. **f** Quantification of alternatively spliced *IL2RG* transcripts by qRT-PCR with two qPCR reactions: Amplification of (3) exon 1–intron 1 and (4) intron 1–exon 2 (***$p \leq 0.001$; 4 independent experiments)

immunoblotting (Supplementary Fig. S1). Moreover, both patients showed no substantial induction of STAT6 phosphorylation upon stimulation with IL-4 (Fig. 3a). These data suggest that the *IL2RG* mutation affects rather selectively IL-4- and IL-21-mediated signaling. This is in line with the observation that T and NK cells are present in normal numbers, whereas class-switched B cells were strikingly reduced.

To gain more insights into structural consequences of the mutations, we modeled wild-type and mutant IL-2Rγ *de novo* and superimposed both structures to IL-2Rγ as part of the IL-2R (PDB: 2B5I), IL-4R (PDB: 3BPL), and IL-15R complexes (PDB: 4GS7) (Fig. 3b) [13–15]. Previous structural and biochemical experiments have highlighted the critical contribution of α-subunits in stabilization of cytokine binding and formation of high affinity complexes for heterotrimeric receptor complexes such as IL-2R and IL-15R [13, 15, 20]. Our analysis predicted a close proximity of the cytokine and the α-subunit with the N-terminal domain of wild-type IL-2Rγ, while the mutant showed a more open conformation which may reduce possible interaction sites with the cytokine and result in weaker binding and lower affinity (Fig. 3b). In contrast, we assume that affinity generated by the interaction of the cytokine and α-subunit in the case of IL-2R and IL-15R is sufficient to stabilize binding and enable signaling for mutant IL-2Rγ in our patients. Corresponding to the impaired IL-4 and IL-21 signaling in both patients, cytokine stabilization via the N-terminal domain of IL-2Rγ might be more critical for the function of heterodimeric IL-4 and IL-21 receptors.

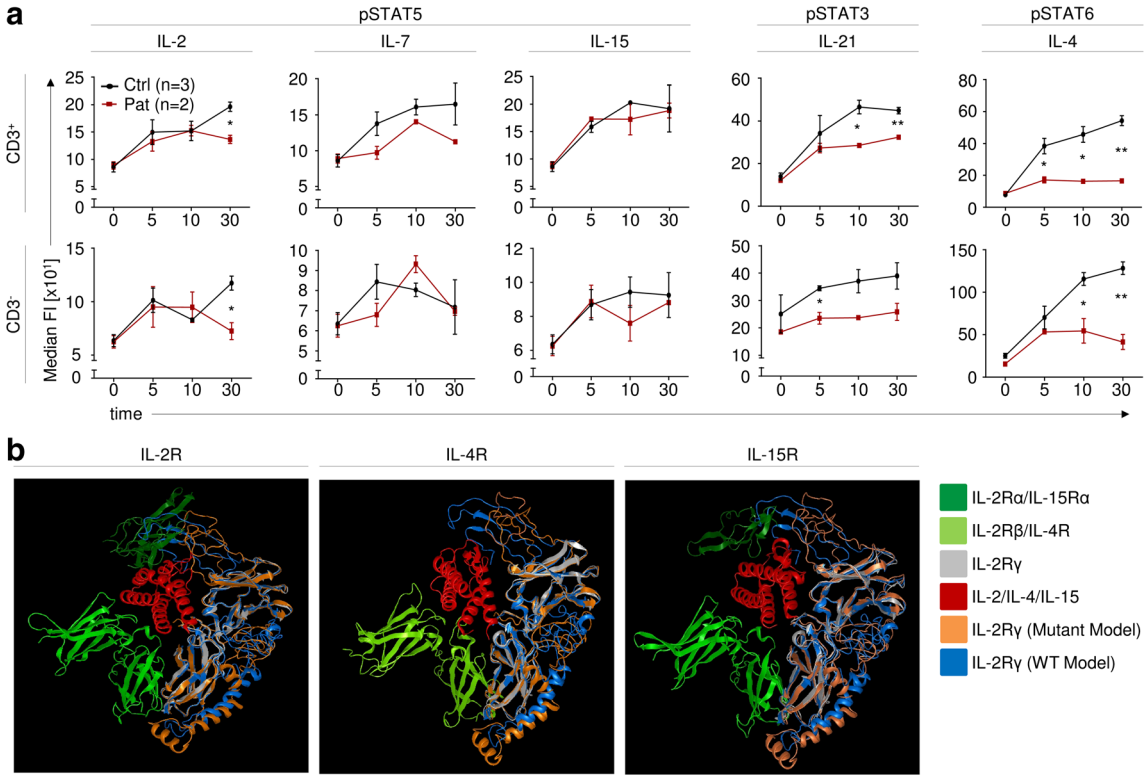

Fig. 3 Distinct IL-2Rγ-mediated downstream signaling defects in patient cells. **a** Representative FACS analysis of phosphorylation of STAT5, STAT3, and STAT6 in $CD3^+$ and $CD3^-$ peripheral blood cells upon stimulation with IL-2, IL-4, IL-7, IL-15, and IL-21 (*$p \leq 0.05$; **$p \leq 0.01$; two independent experiments). **b** Analysis of *de novo* predicted protein structures of WT and mutant IL-2Rγ in comparison to published crystal structures of the IL-2 (PDB: 2B5I [13]), IL-4 (PDB: 3BPL [14]), and IL-15 (PDB: 4GS7 [15]) receptor complexes

Discussion

The clinical diagnosis of atypical SCID remains challenging. Here, we report two patients with a base pair deletion in the *IL2RG* gene suffering from atypical SCID accompanied by chronic cryptosporidiosis, severe diarrhea, and cholangitis. Intriguingly, our patients showed normal T cell frequencies but impaired B cell class switch. Clinical and immunological findings were suggestive of IL-21R deficiency rather than IL-2Rγ deficiency [16]. Our study exemplifies that novel pathomechanisms can result in atypical phenotypes unexpected from the genetic screening.

Differentially impaired cytokine signaling and distinct phenotypes in the case of other *IL2RG* deficiencies have been previously reported [9, 21]. Our patients showed primarily a defective IL-4 and IL-21 signaling, while IL-2, IL-7, and IL-15 signaling were only mildly affected. Abnormal IL-4 and IL-21 signaling is in line with impaired B cell differentiation, and residual IL-2, IL-7, and IL-15 signaling might explain the presence of T and NK cells in our patients. These findings were unexpected based on the predicted deleterious effects of the base pair deletion in *IL2RG*. Functional experiments showed that an alternative splicing mechanism in *IL2RG* bypassed loss of protein expression and led to residual signaling activity.

Differential usage of canonical and alternative splice sites may be considered in other diseases [22]. The canonical 5′ splice site (Fig. 2e) downstream of exon 1 in *IL2RG* is weak, and the mutation may further enhance usage of the alternative site by relaxing RNA structural constraints as indicated by *in silico* RNA structure analysis. Synonymous and intronic mutations are often considered insignificant by many algorithms for analysis of genomic data from patients with primary immunodeficiencies and other rare disorders. However, mutations activating or enforcing cryptic splice sites might result in expression of non-sense transcripts and loss of IL-2Rγ expression.

While the receptor for IL-4, IL-7, and IL-21 are heterodimers composed of γ_c and a second chain (IL-4R, IL-7R, and IL-21R), the heterotrimeric IL-2 and IL-15 receptor complexes are built by three proteins (α-, β-, and γ_c-subunits) [14, 15, 23]. The α-subunit in heterotrimeric receptors was shown to increase the affinity to cytokines thus reducing the threshold for signal activation. Our model suggests that the mutation of the N-terminal domain of IL-2Rγ

in heterodimeric receptors (IL-4 and IL-21) may disturb cytokine binding, whereas the α-subunit in heterotrimeric receptors (IL-2 and IL-15) might compensate in part the alterations of the N-terminal domain. Structural and biochemical data suggest that IL-7 exhibits binding mechanisms and sites distinct from other IL-2Rγ cytokines [24] and that IL-4 and IL-21 share overlapping binding epitopes on IL-2Rγ [25] which might explain the observed differences between IL-4/IL-21 and IL-7 signaling in our patients. Previous studies have shown that B cells from X-SCID patients with abrogated expression of IL-2Rγ are capable of responding to IL-4 via a type II IL-4R complex comprised of IL-4Rα/IL-13R chains [26–28]. Reduced IL-4 signaling in our patients might be potentially explained by competition between mutated IL-2Rγ with IL-13R for IL-4/IL-4Rα in contrast to X-SCID patients with loss of IL-2Rγ expression. However, our current data cannot exclude that interactions between IL-2Rγ and IL-4Rα may be affected by the pathogenic mutation found in the IL-2Rγ of our patients. Further structural and biochemical studies are needed to unravel the function of the N-terminal domain of IL-2Rγ and to assess the modulation of interactions between mutated IL-2Rγ and other receptor subunits. This knowledge might help to evaluate the potential of targeting this domain to differentially modulate γ_c signaling pathways.

Taken together, we here present an unusual mutation in the *IL2RG* gene associated with aberrant splicing and differential effects on IL-2Rγ-dependent cytokine receptor signaling. Our case is exemplifying the need of early diagnosis for patients with life-threatening disease. Whereas next-generation sequencing provides a powerful tool for the discovery of genomic mutations, caution might be raised with respect to unusual variants and molecular pathomechanisms, which might not easily be detected by conventional algorithms.

Acknowledgments Our work is dedicated to the patients who sadly succumbed during the course of our studies. We thank the medical staff at the Departments of Pulmonology, Allergology, Rheumatology and Clinical Immunology and the Referral Center for Pediatric Gastroenterology and Nutrition at the Children's Hospital Zagreb. We acknowledge the assistance of the Next-Generation Sequencing Facility and the Flow Cytometry Core Facility at the Dr. von Hauner Children's Hospital.

Authorship Contributions D.I. designed and conducted experiments and analyzed the data. R.C. supported immunophenotypical analysis. M.N., J.K., I.H., and O.J., recruited and clinically characterized the patients and were critical in the interpretation of the human data. M.Ć. performed histological analysis and J.V. performed pre-transplant hepatological evaluation. M.R. conducted whole-exome sequencing and S.H. performed the bioinformatics analysis of sequencing data. J.B. interpreted splicing mechanisms. C.K. and D.K. conceived the study design, supervised D.I., and recruited study participants. D.I., C.K., and D.K. wrote the draft of the manuscript. All authors interpreted the data and approved the final version of manuscript.

Funding Information This work has been supported by The Leona M. and Harry B. Helmsley Charitable Trust, the Collaborative Research Consortium SFB1054 project A05 (DFG), PID-NET (BMBF), BioSysNet, the European Research Council, the Gottfried–Wilhelm–Leibniz Program (DFG), the DAAD network on 'Rare Diseases and Personalized Therapies', the German Center for Infection Research (DZIF), and the Care-for-Rare Foundation. D.I. was funded by the Hanns-Seidel-Stiftung and received ideational support by the Studienstiftung des deutschen Volkes. D.K. has been a scholar funded by the Else Kröner-Fresenius-Stiftung, the Daimler und Benz Stiftung, and the Reinhard Frank-Stiftung.

Compliance with Ethical Standards

Conflict of Interest The authors declare that they have no conflicts of interest.

References

1. Kalman L, Lindegren ML, Kobrynski L, Vogt R, Hannon H, Howard JT, et al. Mutations in genes required for T-cell development: IL7R, CD45, IL2RG, JAK3, RAG1, RAG2, ARTEMIS, and ADA and severe combined immunodeficiency: HuGE review. Genet Med. 2004;6:16–26.
2. Stephan JL, Vlekova V, Le Deist F, Blanche S, Donadieu J, De Saint-Basile G, et al. Severe combined immunodeficiency: a retrospective single-center study of clinical presentation and outcome in 117 patients. J Pediatr. 1993;123:564–72.
3. Buckley RH, Schiff RI, Schiff SE, Markert ML, Williams LW, Harville TO, et al. Human severe combined immunodeficiency: genetic, phenotypic, and functional diversity in one hundred eight infants. J Pediatr. 1997;130:378–87.
4. Felgentreff K, Perez-Becker R, Speckmann C, Schwarz K, Kalwak K, Markelj G, et al. Clinical and immunological manifestations of patients with atypical severe combined immunodeficiency. Clin Immunol. 2011;141:73–82.
5. Buckley RH. Molecular defects in human severe combined immunodeficiency and approaches to immune reconstitution. Annu Rev Immunol. 2004;22:625–55.
6. Rochman Y, Spolski R, Leonard WJ. New insights into the regulation of T cells by gamma(c) family cytokines. Nat Rev Immunol. 2009;9:480–90.
7. Puck JM, Pepper AE, Henthorn PS, Candotti F, Isakov J, Whitwam T, et al. Mutation analysis of IL2RG in human X-linked severe combined immunodeficiency. Blood. 1997;89:1968–77.
8. Fischer A. Severe combined immunodeficiencies (SCID). Clin Exp Immunol. 2000;122:143–9.
9. Fuchs S, Rensing-Ehl A, Erlacher M, Vraetz T, Hartjes L, Janda A, et al. Patients with T(+)/low NK(+) IL-2 receptor gamma chain deficiency have differentially-impaired cytokine signaling resulting in severe combined immunodeficiency. Eur J Immunol. 2014;44:3129–40.
10. Speckmann C, Pannicke U, Wiech E, Schwarz K, Fisch P, Friedrich W, et al. Clinical and immunologic consequences of a somatic reversion in a patient with X-linked severe combined immunodeficiency. Blood. 2008;112:4090–7.
11. Stephan V, Wahn V, Le Deist F, Dirksen U, Broker B, Muller-Fleckenstein I, et al. Atypical X-linked severe combined immunodeficiency due to possible spontaneous reversion of the genetic defect in T cells. N Engl J Med. 1996;335:1563–7.
12. Kotlarz D, Marquardt B, Baroy T, Lee WS, Konnikova L, Hollizeck S, et al. Human TGF-beta1 deficiency causes severe inflammatory bowel disease and encephalopathy. Nat Genet. 2018;50:344–8.

13. Wang X, Rickert M, Garcia KC. Structure of the quaternary complex of interleukin-2 with its alpha, beta, and gammac receptors. Science. 2005;310:1159–63.
14. LaPorte SL, Juo ZS, Vaclavikova J, Colf LA, Qi X, Heller NM, et al. Molecular and structural basis of cytokine receptor pleiotropy in the interleukin-4/13 system. Cell. 2008;132:259–72.
15. Ring AM, Lin JX, Feng D, Mitra S, Rickert M, Bowman GR, et al. Mechanistic and structural insight into the functional dichotomy between IL-2 and IL-15. Nat Immunol. 2012;13:1187–95.
16. Kotlarz D, Zietara N, Uzel G, Weidemann T, Braun CJ, Diestelhorst J, et al. Loss-of-function mutations in the IL-21 receptor gene cause a primary immunodeficiency syndrome. J Exp Med. 2013;210:433–43.
17. Kochetov AV. Alternative translation start sites and hidden coding potential of eukaryotic mRNAs. Bioessays. 2008;30:683–91.
18. Lalonde S, Stone OA, Lessard S, Lavertu A, Desjardins J, Beaudoin M, et al. Frameshift indels introduced by genome editing can lead to in-frame exon skipping. PLoS One. 2017;12:e0178700.
19. Wada T, Yasui M, Toma T, Nakayama Y, Nishida M, Shimizu M, et al. Detection of T lymphocytes with a second-site mutation in skin lesions of atypical X-linked severe combined immunodeficiency mimicking Omenn syndrome. Blood. 2008;112:1872–5.
20. Stauber DJ, Debler EW, Horton PA, Smith KA, Wilson IA. Crystal structure of the IL-2 signaling complex: paradigm for a heterotrimeric cytokine receptor. Proc Natl Acad Sci U S A. 2006;103:2788–93.
21. Kumaki S, Ishii N, Minegishi M, Tsuchiya S, Cosman D, Sugamura K, et al. Functional role of interleukin-4 (IL-4) and IL-7 in the development of X-linked severe combined immunodeficiency. Blood. 1999;93:607–12.
22. Scotti MM, Swanson MS. RNA mis-splicing in disease. Nat Rev Genet. 2016;17:19–32.
23. Rickert M, Wang X, Boulanger MJ, Goriatcheva N, Garcia KC. The structure of interleukin-2 complexed with its alpha receptor. Science. 2005;308:1477–80.
24. McElroy CA, Dohm JA, Walsh ST. Structural and biophysical studies of the human IL-7/IL-7Ralpha complex. Structure. 2009;17:54–65.
25. Zhang JL, Foster D, Sebald W. Human IL-21 and IL-4 bind to partially overlapping epitopes of common gamma-chain. Biochem Biophys Res Commun. 2003;300:291–6.
26. Matthews DJ, Clark PA, Herbert J, Morgan G, Armitage RJ, Kinnon C, et al. Function of the interleukin-2 (IL-2) receptor gamma-chain in biologic responses of X-linked severe combined immunodeficient B cells to IL-2, IL-4, IL-13, and IL-15. Blood. 1995;85:38–42.
27. Matthews DJ, Hibbert L, Friedrich K, Minty A, Callard RE. X-SCID B cell responses to interleukin-4 and interleukin-13 are mediated by a receptor complex that includes the interleukin-4 receptor alpha chain (p140) but not the gamma c chain. Eur J Immunol. 1997;27:116–21.
28. Lin JX, Migone TS, Tsang M, Friedmann M, Weatherbee JA, Zhou L, et al. The role of shared receptor motifs and common Stat proteins in the generation of cytokine pleiotropy and redundancy by IL-2, IL-4, IL-7, IL-13, and IL-15. Immunity. 1995;2:331–9.